

## Electronic Structure of Noble-Metal-Doped Clathrates with Nanostructure Si-Network

Koji Akai, Kenji Koga, Kazunori Oshiro and Mitsuru Matsuura  
Faculty of engineering, Yamaguchi Univ., Tokiwadai 2-16-1, Ube, Yamaguchichi, Japan  
Fax: 81-836-85-9901, e-mail: akai@po.cc.yamaguchi-u.ac.jp

Electronic structures of Ba-based silicon clathrates doped by noble metal elements  $Ba_8M_6Si_{40}$  ( $M=Cu, Ag, Au$ ) are studied by using the *ab initio* method based on the density functional theory. Calculated properties are following, 1) crystal dimensions and position parameters of atoms, 2) band structures and the electronic density of states.

Key words: Ba-filled Si clathrate, noble-metal doping, electronic structure, thermoelectric power

### 1. INTRODUCTION

Recently group-IV element (Si, Ge, Sn) clathrates have been attracting much attention as candidates of high performance thermoelectric materials and new type superconductors with a complex structure[1,2]. Framework structures of clathrates are composed of distorted tetrahedrons with  $sp^3$ -like bonds. The local structure and the bonding nature are similar to that of cubic diamond materials, but the morphology of crystal structures is much different. A lattice of the type-I clathrate consists of two kinds of nano-polyhedra:  $Si_{20}$ -cage and  $Si_{24}$ -cage that are linked by sharing faces, and a nano-structure network is fabricated. Alkali, alkaline-earth or halogen atoms can be enclosed in cages and many kinds of elements can be substituted for the network sites. The varieties of kinds of doping elements, position of substitution and so on bring to various physical properties in the systems and the possibility of controlling material properties by the nano-structure operations [3].

To obtain high performance thermoelectric materials a phonon glass and electron crystal is demanded[4]. In clathrate compounds caged atoms with large atomic number reduce the lattice thermal conductivity effectively and the  $sp^3$ -network conducts carriers. The thermoelectric figure of merit  $ZT=0.8$  in  $Ba_8Ga_{16}Ge_{30}$  was realized[5], where  $ZT=T\sigma\alpha^2/(\kappa_1+\kappa_2)$ , and  $T$ ,  $\sigma$ ,  $\alpha$ ,  $\kappa_1$  and  $\kappa_2$  are a temperature, an electrical conductivity, a thermoelectric power, a lattice thermal conductivity and an electrical thermal conductivity, respectively. In this material doped Ga controls the carrier concentration. But randomly and heavily doped Ga ions reduce the mobility of carriers. A noble metal or a transition metal doping in Ba-based clathrates is an approach to control band structure and carrier concentration, because the number of valence electrons is much less than of Ga.

Noble metal doped clathrates  $Ba_8M_6Si_{40}$  ( $M=Cu, Ag, Au$ ) are the type-I clathrate structure characterized by the space group  $Pm-3n$ , and the noble-metal compounds were synthesized by some authors[6,7,8]. Some noble-metal doped materials show a superconductivity at several K[6] and electrical or thermal properties were measured[9,10].

Our purpose of this study is to calculate the electronic

structures of  $Ba_8M_6Si_{40}$  ( $M=Cu, Ag, Au$ ) by using the *ab initio* method and to discuss an influence of noble-metal-doping to the electronic transport properties from the point of view of the electronic structure.

### 2. COMPUTATIONAL DETAILS

#### 2.1 Electronic structure

Electronic structures are calculated by the Full-Potential linearized augmented plane-wave (FLAPW) method with a generalized gradient approximation (GGA)[11]. The basis functions, i.e. the LAPWs, are composed of linear combinations of an APW and a local orbital (LO)[12]. In the present calculation the WIEN2K package is used[13]. The exchange-correlation potential parameterized by Perdew-Bruke-Enzerhof is used[14]. The cutoff energy of plane waves is 14.5Ry in all the calculating materials. The maximum magnitude of the reciprocal lattice vector  $G$  which is used in the Fourier expansion of charge density is 14/a.u. In this study the following radii of atomic spheres are taken; Ba: 3.0a.u., Si: 2.1a.u., Cu: 2.2a.u., Ag: 2.4a.u., Au: 2.4a.u. In the self-consistent

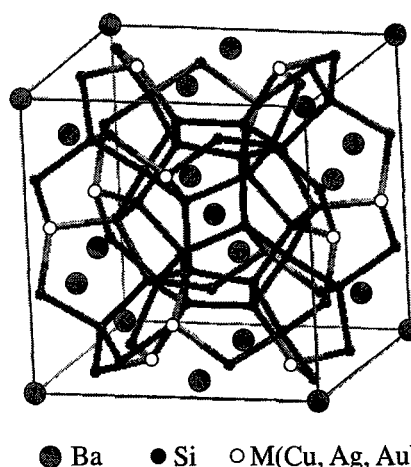


Fig. 1 Crystal structure of  $Ba_8M_6Si_{40}$ . A gray and large circle is Ba atom, a black and small circle is Si atom, and a white and small circle is a noble-metal atom.[17]

field(SCF) calculation to solve the Kohn-Sham equation, 20  $k$ -points are taken in an irreducible Brillouin zone (IBZ) for sampling. To calculate the density of states (DOS) 84  $k$ -points are taken in the IBZ.

## 2.2 Optimization of lattice parameters

A volume and atomic positions are optimized by using the *ab initio* calculation. This procedure consists of two steps. In the first step, the volume optimization is done. In the next step, atomic positions are determined.

The total energy as a function of volume  $V$  is given empirically as [15]:

$$E_{\text{tot}}(V) = c_1 V^{-\alpha} + c_2 V + c_3, \\ V_0 = \left( \frac{c_1(1-\alpha)}{c_2} \right)^{1/\alpha}, \quad B = c_2 \alpha, \quad (1)$$

where  $c_1$ ,  $c_2$ ,  $c_3$ ,  $\alpha$  are fitting parameters determined from the least square fitting,  $V_0$  is an equilibrium volume and  $B$  is a bulk modulus. The lattice constant  $a$  is obtained from  $V_0^{1/3}$ .

Atomic positions are relaxed within the same crystal symmetry and determined by a Newton method. To calculate an atomic force, the Hellmann-Feynman force and the incomplete-basis-set corrections are taken account [16]. The convergence condition of atomic forces is taken at 0.5 Ry/a.u.

## 3. RESULTS AND DISCUSSION

### 3.1 Crystal dimensions and lattice parameters

In the  $\text{Ba}_8\text{Si}_{46}$  lattice there are five different symmetry positions:  $2a$ ,  $6d$  that are occupied by Ba atoms and  $6c$ ,  $16i$ ,  $24k$  that are occupied by Si atoms. When transition elements or noble metal elements are doped in  $\text{Ba}_8\text{Si}_{46}$ , doped atoms occupy at  $6c$  sites selectively [18, 19, 20]. Figure 1 shows a unit cell of  $\text{Ba}_8M_6\text{Si}_{40}$  ( $M=\text{Cu}, \text{Ag}, \text{Au}$ ). A gray and large circle denotes a Ba atom, a black and small circle denotes a Si atom, a white and small circle denotes a noble-metal atom. Positions of  $2a$  sites are the center and the corner of the unit cell. A  $2a$  site is in a dodecahedral  $\text{Si}_{20}$ -cluster which is composed of  $16i$  sites and  $24k$  sites.  $\text{Si}_{20}$ -clusters make a fcc lattice and each Si cluster contacts at  $16i$  sites. Ba atoms at  $6d$  sites and noble-metal atoms at  $6c$  sites are in the interstitial region among  $\text{Si}_{20}$  clusters and a  $6d$  site and a  $6c$  site are a neighborhood.

Those five kinds of atomic positions are characterized by the following Wyckoff parameters:  $2a:(0,0,0)$ ,  $6d(0.25,0.5,0)$ ,  $6c(0.5,0.25,0)$ ,  $16i(x,x,x)$ ,  $24k(0,y,z)$ . Positional parameters ( $x, y, z$ ) and a lattice parameter  $a$  are not determined from the space group symmetry. These lattice parameters are computed by the *ab initio* calculation. Table I is a list of the lattice parameters and the bulk modulus of  $\text{Ba}_8M_6\text{Si}_{40}$  ( $M=\text{Cu}, \text{Ag}, \text{Au}$ ). The result of lattice constants shows that the lattice constant of the Ag compound is the largest of the three compounds. This is in agreement with the tendency of experimental results. All of lattice constants obtained by the SCF calculation are slightly larger than those of experimental values, *i.e.* these differences are 0.8% (Cu), 1.1% (Ag), 1.1% (Au). In general, as the GGA gives a larger value about 0.5% than the experimental value for a lattice constant, the difference between theory and experiment is reasonable.

In noble-metal-doped Si clathrates, the measurement

Table I Lattice parameters of type I clathrates  $\text{Ba}_8M_6\text{Si}_{40}$ .  $a$  is a lattice constant,  $x$  is a position parameter at a  $16i$  site,  $y$  and  $z$  are position parameters at a  $24k$  site.  $B$  is bulk modulus.

a. $\text{Ba}_8\text{Cu}_6\text{Si}_{40}$					
	$a(\text{\AA})$	$x$	$y$	$z$	$B(\text{GPa})$
SCF	10.41	0.183	0.311	0.119	74.9
Exp. <sup>[6]</sup>	10.34				
b. $\text{Ba}_8\text{Ag}_6\text{Si}_{40}$					
SCF	10.56	0.184	0.302	0.115	71.5
Exp. <sup>[6]</sup>	10.45				
c. $\text{Ba}_8\text{Au}_6\text{Si}_{40}$					
SCF	10.53	0.184	0.304	0.117	78.9
Exp. <sup>[8]</sup>	10.42	0.183	0.31	0.166	

of a bulk modulus is not reported. But in  $\text{K}_8\text{Si}_{46}$  volume dependence of pressure was measured [21]. From the result, the bulk modulus is estimated to be 88 GPa. Reny *et al.* measured the density of states of phonons for several Si clathrates by using the neutron scattering method [10]. The results of their measurements show that the Debye energy of  $\text{Ba}_8\text{Ag}_6\text{Si}_{40}$  is similar to that of  $\text{K}_8\text{Si}_{46}$ . From these results, we can guess that the value of bulk modulus on  $\text{Ba}_8\text{Ag}_6\text{Si}_{40}$  is of the order of that of  $\text{K}_8\text{Si}_{46}$  and the calculated results of bulk modulus are reasonable. A sound speed of the longitudinal acoustic mode can be estimated from the relation  $c = \sqrt{B/\rho}$  roughly, where  $\rho$  is a density of mass. The sound speeds of the clathrate compounds are obtained as  $4.4 \times 10^3$  m/s in  $\text{Ba}_8\text{Cu}_6\text{Si}_{40}$ ,  $4.2 \times 10^3$  m/s in  $\text{Ba}_8\text{Ag}_6\text{Si}_{40}$  and  $4.04 \times 10^3$  m/s in  $\text{Ba}_8\text{Au}_6\text{Si}_{40}$ , respectively.

### 3.2 Band structure

Band structures and the DOS of  $\text{Ba}_8M_6\text{Si}_{40}$  are shown in Fig. 3, then the unit of DOS is states/eV·cell. A broken line denotes Fermi level. To compare with results for the noble-metal compounds the band structure and the DOS of  $\text{Ba}_8\text{Si}_{46}$  are shown in Fig. 3d. The lattice parameters are the same as of  $\text{Ba}_8\text{Au}_6\text{Si}_{40}$ . Figure 4 shows the partial DOS of each  $s$ ,  $p$ ,  $d$  orbital on an Au-atom. A solid line is a  $s$ -orbital component, a dotted line is  $p$ , a solid line with crosses is  $d$ .

In  $\text{Ba}_8\text{Si}_{46}$  the band structure is composed of three parts; the lowest energy part from about  $-13$  eV to  $-5$  eV which is Si:  $s$ -like band, the middle energy part from  $-5$  eV to  $-1$  eV which is Si:  $p$ -like band, and the higher energy part which is the conduction band over  $-1$  eV. The conduction band hybridizes with Ba  $sd$ -orbital and anti-bonding Si  $p$ -orbital. This overall structure is also seen in the noble-metal compounds. The large DOS is seen in the middle energy part or at an intersection between the lowest energy part and the middle energy part, which is characterized by  $d$ -bands of the noble metal elements. The center energy of the  $d$ -bands is  $-3$  eV and the band width is about 2 eV in  $\text{Ba}_8\text{Cu}_6\text{Si}_{40}$ ,  $-5$  eV and 2 eV in  $\text{Ba}_8\text{Ag}_6\text{Si}_{40}$ ,  $-5$  eV and 3 eV in  $\text{Ba}_8\text{Au}_6\text{Si}_{40}$ , respectively. From a viewpoint of the  $d$ -orbital radius we think that the band width in  $\text{Ba}_8\text{Ag}_6\text{Si}_{40}$  should become larger than that in  $\text{Ba}_8\text{Cu}_6\text{Si}_{40}$ , but it is reasonable from the lattice size. Because the  $d$ -orbital is localized and the lattice constant in  $\text{Ba}_8\text{Ag}_6\text{Si}_{40}$  is the largest in the three

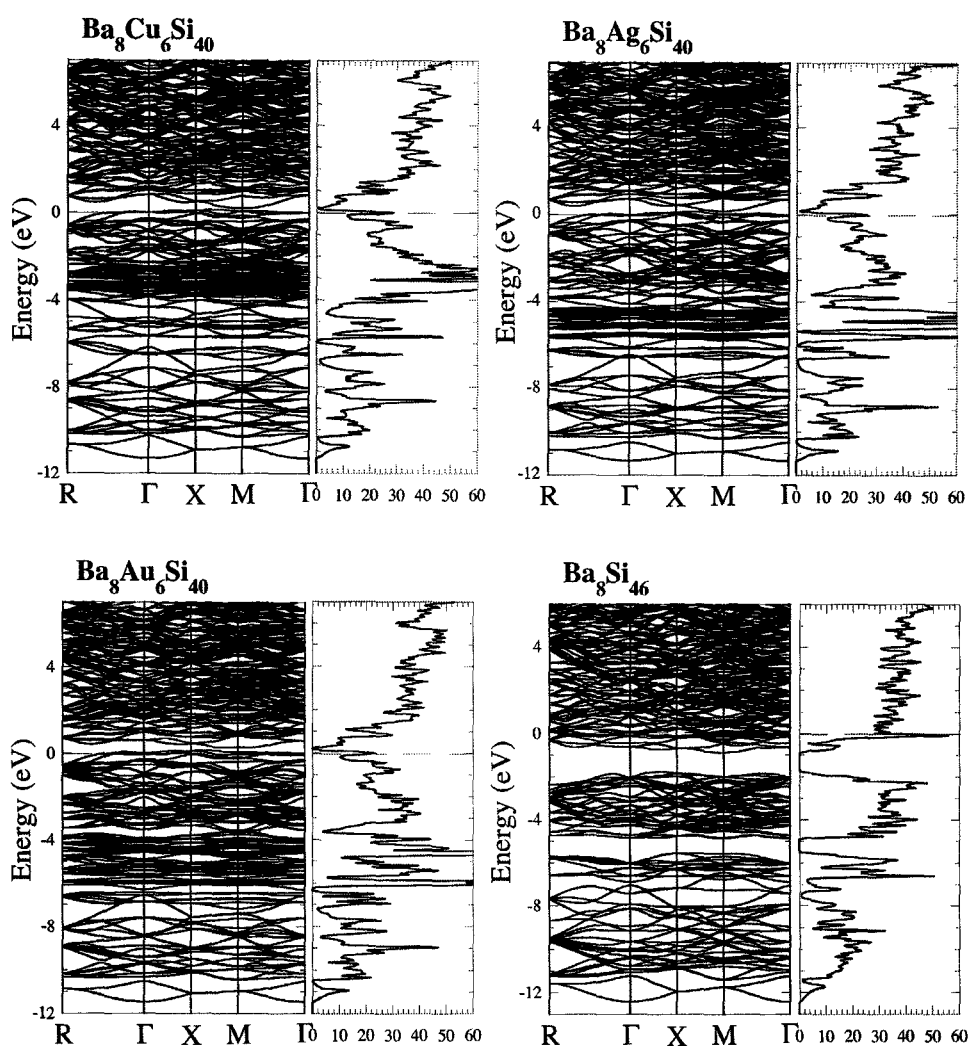


Fig. 3 Band structures and DOS of  $Ba_8M_6Si_{40}$ , a)  $M=Cu$ , b)  $M=Ag$ , c)  $M=Au$ , d)  $Ba_8Si_{46}$ . The unit of the DOS is States/eV. A broken line denotes the Fermi level.

clathrates. This fact suggests that bonding between a noble-metal atom and a Si atom is mainly characterized by  $sp$ -orbitals on the noble metal atom.

In the DOS of the middle energy part for  $Ba_8Ag_6Si_{40}$  and  $Ba_8Au_6Si_{40}$  a double peaks structure appears. This structure is due to a difference of each atomic characters. In Fig. 4 it is seen that the Au:  $p$ -orbital contributes to the higher energy peak and is less contribution for the lower energy peak, and vice versa for the  $s$ -orbital. In addition the Si:  $p$ -orbital at 16i sites has large contribution for the lower energy peak.  $Ba_8Cu_6Si_{40}$  has also the double peak structure, but due to the large DOS of 3d-bands the structure is covered.

As the electronic structure near Fermi energy is significant for thermoelectric properties and transport properties, we focus to this electronic structure. The DOS near the Fermi level has a sharp peak due to the flat bands. The origin of these bands can be understood from the partial DOS. The sum of partial DOS on each atoms is obtained in  $Ba_8Au_6Si_{40}$  as; Ba(2a): 0.54, Ba(6d): 0.57, Au(6c): 2.7, Si(16i): 3.1, Si(24k): 5.4. It indicates that the flat bands are characterized by the

$d$ -orbital on Ba atoms and the  $p$ -orbital on the framework atoms. These orbitals make a mixing band.

Concerned to the effects of Au atom it is shown in Fig. 4. As seen in this figure, the partial DOS for the  $d$ -orbital has the largest magnitude in the wide range. But at the Fermi level the partial DOS of the  $p$ -orbital is comparable with of the  $d$ -orbital. It indicates that the dominant contribution to the electronic properties is due to the  $p$ -orbital, because the  $d$ -orbital wave function is localized much strongly compared with the  $p$ -orbital wave function.

The Fermi DOS  $\rho_F$  of  $Ba_8M_6Si_{40}$  is obtained from Fig. 3 as:  $\rho_F=32(Ba_8Cu_6Si_{40})$ ,  $\rho_F=27(Ba_8Ag_6Si_{40})$ ,  $\rho_F=25(Ba_8Au_6Si_{40})$ , the unit is states/eV. For  $Ba_8Au_6Si_{40}$ , Kawaguchi *et al.* measured the magnetic susceptibility and estimated the Pauli paramagnetic susceptibility  $\chi_P$  as 1.42emu/g[7]. By using the relation  $\chi_P=(g\mu_B/2)^2\rho_F$ , the DOS of the experimental value is obtained as  $\rho_F^{(exp)}=15\text{states/eV}$ . This value is about half of the theoretical one. The reason of this disagreement is unknown.

The six bands from the 339th to the 344th are across

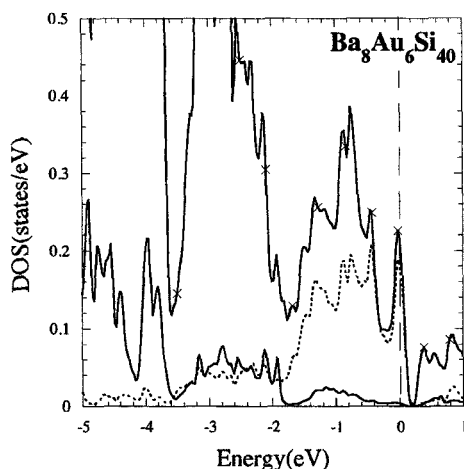


Fig. 3 Partial DOS with Au: *s*, *p*, *d* characters in  $\text{Ba}_8\text{Au}_6\text{Si}_{40}$  near Fermi level. A solid line is *s* component, a dotted line is *p*, a solid line with cross hatches is *d*. A broken line denotes Fermi level.

over the Fermi level in all of the calculated clathrates. These bands lie just under the band gap as seen in Fig. 3. The clathrate  $\text{Si}_{46}$  is a semiconductor with a wide gap. The same order band gap is seen in the band structure of  $\text{Ba}_8\text{Si}_{46}$ . In  $\text{Ba}_8\text{Si}_{46}$  Ba atoms act donors with two excess electrons and the Fermi level is raised into the conduction band. In the present calculation the number of valence electrons is 342 for  $M=\text{Cu}$ ,  $\text{Ag}$  and  $\text{Au}$ . As the 344th band is the top of valence band,  $\text{Ba}_8M_6\text{Si}_{40}$  system has two holes in a unit cell. It indicates that a doped atom,  $\text{Cu}$ ,  $\text{Ag}$ ,  $\text{Au}$ , acts an acceptor in the clathrates and supplies to four holes. This conclusion is also supported by the results of the partial DOS calculation for  $\text{Cu}$ ,  $\text{Ag}$ ,  $\text{Au}$ . Because in Fig. 4 the *p*-orbital component is dominant under the gap and this is similar to the DOS configuration for  $\text{Si}(6c)$  *p*-orbital in  $\text{Ba}_8\text{Si}_{46}$ .

From the viewpoint of carrier doping to clathrate, the noble-metal clathrate compounds are able to be regard as degenerate semiconductors. The carrier density in the materials is of the order of  $2 \times 10^{21} \text{cm}^{-3}$  and it is low comparison with of usual metals. Then  $\text{Ba}_8M_6\text{Si}_{40}$  are indirect semiconductors; the top of valence band is located on the XM line(T) and the bottom of conduction band is located on the M point in  $\text{Ba}_8\text{Cu}_6\text{Si}_4$  and  $\text{Ba}_8\text{Ag}_6\text{Si}_4$  and on the XM line(T) in  $\text{Ba}_8\text{Au}_6\text{Si}_4$ . The band gap energy of each material is 64meV in  $\text{Ba}_8\text{Cu}_6\text{Si}_{40}$ , 48meV in  $\text{Ba}_8\text{Ag}_6\text{Si}_{40}$ , 144meV in  $\text{Ba}_8\text{Au}_6\text{Si}_{40}$ . Those gap energies are much smaller than that of  $\text{Ba}_8\text{Si}_{46}$ .

#### 4. SUMMARY

We studied the electronic structures of the noble-metal-doping type-I clathrate compounds  $\text{Ba}_8M_6\text{Si}_{40}$  ( $M=\text{Cu}$ ,  $\text{Ag}$ ,  $\text{Au}$ ) by using the FLAPW-GGA method.

The lattice constants and crystal parameters were calculated by using the method. The results agree with experimental values within the difference of 1%.

The calculated band structure and the density of states of all of the compounds are similar to that of  $\text{Ba}_8\text{Si}_{46}$  in the overall energy range, except for the *d*-bands of noble metal atoms. Their *d*-bands lie in the energy ranges from

$-3\text{eV}$  to  $-5\text{eV}$ , thus the *d*-band effects near the Fermi level is small and the dominant contributions to transport properties are brought by the *p*-orbital. The *p*-orbital overlaps with Si: *sp*-orbitals at the nearest neighbor sites and those orbitals consist of covalent bonds. It was shown that a doped noble-metal-atom acts an donor with four holes.

At the Fermi level four flat bands exist and make a peak structure for the DOS. Their bands are mainly characterized by Ba *5d*-orbitals at 2a sites.

#### 5. REFERENCES

- [1] G. S. Nolas, G. A. Slack and S. B. Schujman, "Recent Trends in Thermoelectric Materials Research I", Edit. T. M. Tritt, Academic Press (2001).
- [2] H. Kawaji, H. Horie, S. Yamanaka and M. Ishikawa, Phys. Rev. Lett., **20**(1995), 1427.
- [3] W. Lek NG, M. A. Lourenco, R. M. G. William, S. Ledain, G. Shao and K. P. Homewood, Nature(London) **410**(2001), 192.
- [4] B. C. Sales, D. Mandrus, B. C. Chakoumakos, V. Keppens, and J. R. Thompson, Phys. Rev. **B56** (1997), 15081.
- [5] N. Nakagawa, M. Miyake, H. Hayase and T. Koyanagi, (private communication, to be published).
- [6] R. F. W. Herrmann, K. Tanigaki, S. Kuroshima, H. Suematsu, Chem. Phys. Lett. **283**(1998), 29.
- [7] G. Cordir and P. Woll, J. Less-Common Met. **169**(1991), 291.
- [8] R. F. W. Herrmann, K. Tanigaki, T. Kawaguchi, S. Kuroshima and O. Zhou, Phys. Rev. **B60**(1999), 13243
- [9] H. Sakamoto, H. Tou, H. Ishii, Y. Maniwa, E. A. Reny and S. Yamanaka, Physica **C341-348**(2000), 2135.
- [10] E. Reny, A. San-Miguel, Y. Guyot, B. Masenelli, P. Melinon, L. Saiot, S. Yamanaka, B. Champagnon, C. Cros, M. Pouchard, M. Borowski and A. J. Dianoux, Phys. Rev. **B66**(2002), 014532.
- [11] D. J. Singh, "Planewaves, Pseudopotentials and the LAPW Methods", Kluwer Academic Publishers (1994).
- [12] E. Sjustedt, L. Nordstrom, D. J. Singh, Solid State Comm., **114**, 15(2000)
- [13] P. Blaha, K. Schwarz, G. Madsen, D. Kvasnica and J. Luitz, program package WIEN2K, Technical University of Vienna (2001).
- [14] J. P. Perdew, S. Burke and M. Ernzerhof, Phys. Rev. **B45**, 3865(1996).
- [15] F. D. Murnaghan, Proc. Natl. Acad. Sci. U.S.A. **30**, 244(1944).
- [16] R. Yu, D. Singh and H. Krakauer, Phys. Rev. **B43**, 6411(1991)
- [17] A. Kokalj, J. Mol. Graphics Modelling, **17**(1999), 176.
- [18] T. Kawaguchi, K. Tanigaki and M. Yasukawa, Appl. Phys. Lett., **77**(2000), 3438.
- [19] Y. Mudryk, P. Rogl, C. Paul, S. Berger, E. Bauer, G. Hilsher, C. Godart, H. Noel, A. Saccone and R. Ferro, Physica B, **328**(2003), 44.
- [20] T. Kawaguchi, K. Tanigaki and M. Yasukawa, Phys. Rev. Lett., **85**(2000), 3189.
- [21] J. S. Tes, S. Desgreniers, Z. Li, M. R. Ferguson and Y. Kawasoe, Phys. Rev. Lett. **89**(2002), 195507.